A R C H I V E S O F M E T A L L U R G Y A N D M A T E R I A L S
Volume 60 2015 Issue 3
DOI: 10.1515/amm-2015-0382

D. KOPYCIŃSKI*#, E. GUZIK*

# FLUX EFFECT ONTO PERITECTIC PHASES GROWTH IN THE ZINC COATING

# WPŁYW TOPNIKA NA WZROST FAZ PERYTEKTYCZNYCH W POWŁOCE CYNKOWEJ

A model of the (Zn) – coating formation on the iron/steel substrate is proposed. The model assumes the phases' sub-layers creation in a sequence. This sequence is referred to the Fe-Zn phase diagram. However, this sequence of phases' appearance is perturbed by the flux presence in the zinc bath. The flux effect on the coating morphology and appearance/disappearing of some sub-layers is analysed. The phases' formation is treated as the result of the peritectic reaction accompanying the coating solidification. A comparison of the coating formations before and after flux decay is delivered. Thus, a function which describes the flux decay is also analysed. Additionally, a ternary Fe-Zn-F(flux) phase diagram is considered. The varying zinc concentration across the phases sub-layers is described with the use of the function which determines the flux decay. The behaviour of the solidification path before and after flux decay is discussed due to the adequate equations formulated in frame of the current model.

*Keywords:* Fe-Zn-flux phase diagram; flux disappearing; coating thickening

Zaproponowany został model kształtowania się powłoki (Zn) na podłożu ze stali/żelaza. Model zakłada powstawanie podwarstw faz w pewnej sekwencji. Sekwencja ta odniesiona jest do diagramu równowagowego. Jednak, sekwencja ta zakłócona jest obecnością topnika w kąpieli. Wpływ topnika na morfologię powłoki oraz na pojawianie się/zanik niektórych podwarstw jest analizowany. Powstawanie faz traktowane jest jako rezultat reakcji perytektycznych towarzyszących krystalizacji powłoki. Pokazane jest porównanie kształtowania się powłoki przed i po zaniku topnika. Stąd, analizowana jest również funkcja, która opisuje zanik topnika. Dodatkowo, rozważany jest potrójny diagram fazowy Fe-Zn-topnik. Zmienne stężenie cynku na grubości podwarstw opisane jest z użyciem funkcji, która opisuje zanik topnika. Zachowanie się ścieżki krystalizacji przed i po zaniku topnika jest dyskutowane w odniesieniu do stosownych równań sformułowanych w proponowanym modelu.

## 1. Introduction

Technology of the hot-dip galvanizing requires to apply a flux which is able to improve the adhesion of the (Zn) – coating settled on the steel substrate, [1-11]. As the (Zn) – coating consists of two layers: first layer being directly in the contact with substrate and second layer being the result of the substrate/coating system emerging from the zinc bath, the adhesion between substrate and first layer is of the main significance for the technology, [12-15].

Therefore, the $\Gamma_1$ and $\delta$ – phases appearance is the subject of the critical analysis in the current approach. However, other phases formation, like $\zeta$ or $\zeta_Z \equiv \zeta + \eta$ will also be considered, especially in the agreement with the solidification sequence resulting from the phase diagram, as discussed in literature, [16,17].

## 2. Model for the zinc coating growth

A schematic model for the sub-layers formation in the zinc coating is shown in Fig. 1. It results from this scheme that the sub-layers appear in the coating sequentially. Each sub-layer phase is the product of the peritectic transformation under non-equilibrium condition, that is due to undercooled peritectic reaction.

The solidification accompanied by peritectic reaction is preceded by the substrate dissolution within the zone denoted *dx*, to produce the $N_0^F$ – liquid solution, Fig. 1. It occurs according to the reaction: $liquid\,(N^F)$ + Fe → $liquid\,(N_0^F)$.

* AGH UNIVERSITY OF SCIENCE AND TECHNOLOGY, FACULTY OF FOUNDRY ENGINEERING, 23 REYMONTA STR., 30-059 KRAKÓW, POLAND
# Corrersponding author:djk@agh.edu.pl

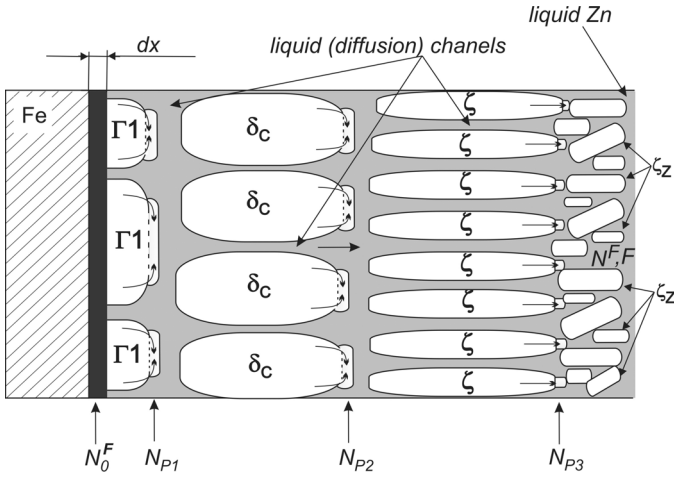


Fig. 1. Model for the cyclic substrate dissolution in the zone, *dx*, and solidification with marked course of the peritectic reactions; the $N_{Pi}$ – solute concentrations ($i = 1, ..., q$) indicate the localization of the adequate peritectic reaction leading to the phase sub-layer thickening; channels are used for the liquid zinc (its equilibrium solution, $N^F$, in fact) diffusion towards the dissolution zone in the substrate

At the beginning of the zinc coating formation the neighboring bath contains: Zn + F (flux), Fig. 2a. Next, the *dx* – dissolution zone is created by the reaction: *liquid* (Zn) + Fe → *liquid* ($N_0^F$), Fig. 2b. The liquid from the *dx* – dissolution zone diffuses towards the bath to promote two first sub-layers formation due to peritectic reaction: $\alpha$ + *liquid* ($N_1$) → $\Gamma_1$ which is followed by the subsequent in sequence peritectic reaction: $\Gamma_1$ + *liquid* ($N_2$) → $\delta$, ($\delta \equiv \delta_C$, in fact), Fig. 2c. At the same time the remaining liquid enters into the reaction with the zinc to transform it into its equilibrium solution: *liquid* ($N_2$) + *liquid* (Zn) → *liquid* ($N^F$).

Now, the $N^F$- equilibrium zinc solution forms the liquid in the *dx* – dissolution zone according to the reaction: *liquid* ($N^F$) + Fe → *liquid* ($N_0^F$), as mentioned above, Fig. 2d. Simultaneously, the birth/nucleation of the $\delta_P$ – phase occurs on the previously formed $\delta_C$ – phase sub-layer, when solidification time is: $t = t_C$, Fig. 2d. Nothing opposites to the $\zeta$ – phase appearing which forms two sub-layers: $\zeta$ – itself and $\zeta_Z \equiv \zeta + \eta$, Fig. 2d. At the $t_C$ – time the flux disappears/decays and the growth of the $\delta_C$ – phase sub-layer is arrested. Instead, the $\delta_P$ – phase sub-layer is formed, exclusively, Fig. 2e. Now, the Zn – solute concentration in the dissolution zone attains a new value: $N_0^F \rightarrow N_0$, which occurred at time $t = t_C$, Fig. 2d, Fig. 2e.

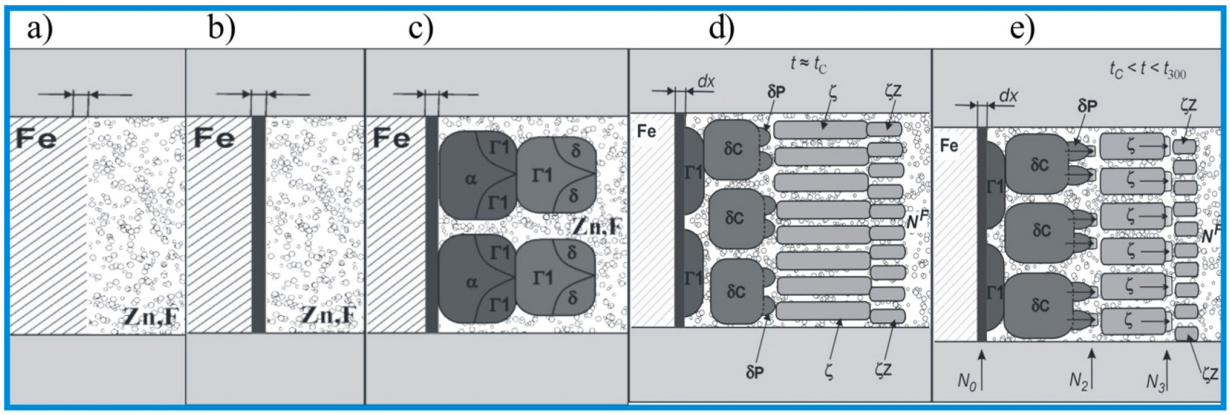


Fig. 2. Model for sequential occurrence of phenomena taking part during the (Zn) – coating formation on the steel substrate; schemes a/ b/ c/ correspond to the first 13 seconds of the process under investigation; $t_C$ = 150 seconds (scheme d/); fully developed galvanizing process occurs when the flux is evaporated, that is for $t > t_C$, (scheme e/); $t_M \approx 300$ seconds

All the phenomena discussed above, Fig. 2, can be related to the Fe-Zn phase diagram. Recently, a new phase diagram has been published, [18]. This phase diagram is exclusively dedicated to the hot dip galvanizing technology, Fig. 3. The $T_R$ – real temperature of the hot dip galvanizing is superimposed on the diagram. Also, the $N_0^F$ – solute concentration, typical for the beginning of the galvanizing, (described in Fig. 1) is marked in the phase diagram, Fig. 3. As the peritectic transformations occur at the $T_R$ – real temperature they become the undercooled peritectic reactions. The solidification is isothermal one due to the imposed real temperature and therefore, the Number of the Degree of Freedom is equal to zero. In fact, $f = c + 1 = 0$ with $c$ = Fe, Zn, F (*flux*); $p$ = *liquid* ($N_0^F$), $\Gamma_1$, $\delta$, $\zeta$, (where flux consists of Zn and Cl)

It is assumed, in the first approximation, that the intersection of the $T_R$ – real temperature with the *liquidus* line defines the end of solidification path denoted as $N^F$, Fig. 3. Strictly analyzing, the $N^F$ equilibrium solution of the iron in zinc results from the intersection of the $T_{Zn}^m$ – isotherm with the liquidus line, [19,20], ($T_{Zn}^m$ – the melting point of zinc). So, the length of the solidification path is $N_0^F \div N^F$ within the period of time when the flux is not yet evaporated, Fig. 3.

It seems that the formation of channels used by this system for the boundary diffusion is a natural phenomenon accompanying the peritectic reaction. Various issues related with the peritectic solidification were described in detail in literature, [21]. An important case of the peritectic solidification is the situation when the primary $\alpha$ phase is not a substrate for the nucleation of the $\beta$ – phase, Fig. 4a. Then, the $\beta$ – peritectic phase nucleates in the liquid surrounding the $\alpha$ – phase. The concentration of the liquid surrounding the $\alpha$ – phase changes during the

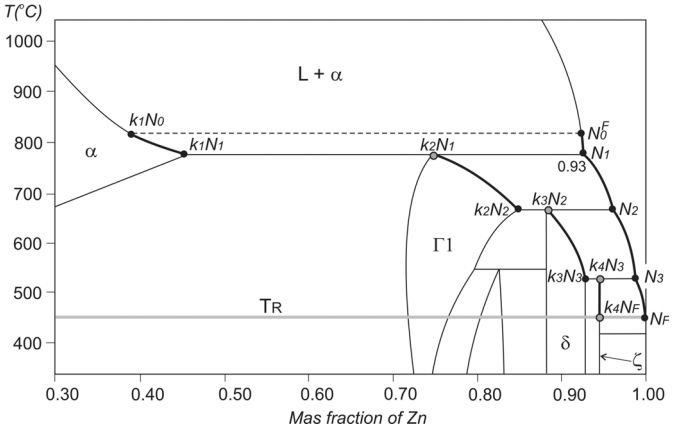


Fig. 3. Fe-Zn phase diagram for stable equilibrium, [18]; some parameters used in the current description are marked; ($k_i$; $i$ = 1,…,$q$ is the partition ratio in the solidification ranges appearing in sequence according to a given phase diagram)

growth of the $\beta$ – phase. Finally, the adequate thermodynamic conditions are created to promote melting of the $\alpha$ – phase and further growth of the $\beta$ – phase, [20]. This process of peritectic phase formation is called the peritectic reaction (as opposed to peritectic transformation shown in Fig. 4b).

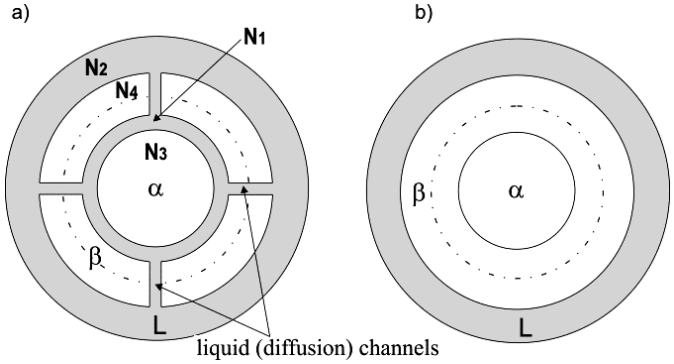


Fig. 4. Schematic diagram for: a/ peritectic reaction, b/ peritectic transformation, [20]

### 3. Flux effect onto the (Zn) – coating formation

The contribution of the third component which is flux designated as $F$, to the hot dip galvanizing technology, is to be examined in order to describe the solidification process under investigation. It is the presence of the $F$ – flux in the galvanizing that makes the $\Gamma_1$ – phase growth and, as mentioned above, also promotes the appearance of the $\delta_c$ – phase of the compact morphology, [22].

The model also assumed that the $\zeta_Z$ – phase sub-layer stops growing at the $t_C$ – time, that is, at an instant when the decay of flux and products of its combustion/decomposition which evaporate is completed, Fig. 5. Further extension of the model, to better its adaptation to the needs of the galvanizing technology, requires the development of a hypothesis regarding the flux life in the process. It has been assumed with good result, after comparing the simulation with measurement, that 90% of the flux fades immediately upon being introduced to the zinc bath. The remaining 10% (or 0.1 in mass fraction) is actively involved in the process of solidification, Fig. 6.

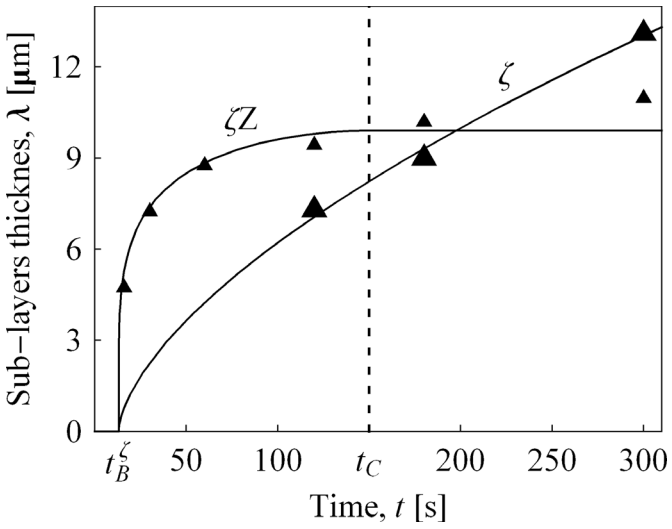


Fig. 5. Highlighting the differences between the kinetics of the $\zeta$ – phase sub-layer growth and of the $\zeta_Z$ – sub-layer appearing / disappearing (oscillation)

Hypothetical function which describes the flux behavior in the process of the (Zn) – coating growth on iron, Fig. 6 has three characteristic points (indicated by dots): the first – for the time, $t_B^{\Gamma_1}$ (birth of the $\Gamma_1$ – phase), the second – for the time, $t_B^\zeta$ (birth of the $\zeta$ – phase) and the third – for the $t_C$ – time. It allows for defining the $F(t)$ – function which describes the flux evaporation, Eq. (1).

The process of flux decay was divided into two phenomena: burning out of the flux and the effect of combustion products on the coating solidification. Both phenomena are juxtaposed, and the resultant hyperbole, $F(t)$, could be plotted hypothetically, Fig. 6.

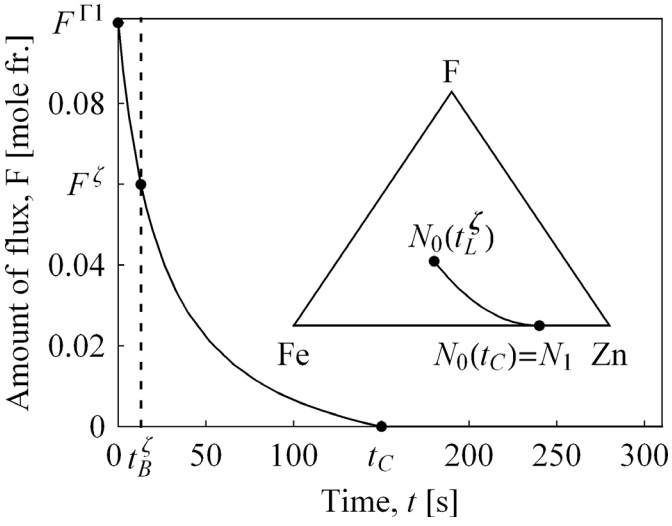


Fig. 6. Hypothetical function describing the flux behavior in the (Zn) – coating growth on the *Armco* iron – substrate; the (Fe-Zn-F) – virtual ternary phase diagram is also delivered.

$$F(t)=\frac{t-t_C}{a\,t+b},\qquad t_B^{\Gamma 1}\le t \tag{1}$$

$$a=\frac{t_B^{\Gamma 1}F^{\zeta}-t_B^{\zeta}F^{\Gamma 1}+t_C F^{\Gamma 1}-t_C F^{\zeta}}{F^{\Gamma 1}F^{\zeta}\,(t_B^{\Gamma 1}-t_B^{\zeta})}=-60.2\ ;$$

$$b=\frac{t_B^{\Gamma 1}\,t_B^{\lambda}\,(F^{\Gamma 1}-F^{\zeta})+t_C\,(t_B^{\zeta}\,F^{\zeta}-t_B^{\Gamma 1}\,F^{\Gamma 1})}{F^{\Gamma 1}F^{\zeta}\,(t_B^{\Gamma 1}-t_B^{\zeta})}=-1500$$

The above function, Eq. (1), requires the selection of the parameters such as: $F(t_B^{\Gamma_1})\equiv F^{\Gamma_1}$ and $F(t_B^{\zeta})\equiv F^{\zeta}$, Fig. 6, to make the model coherent in confrontation with the measurements of the $N(\lambda)$ – solute concentration. Additionally, the $t_C$ – parameter is also to be known, and can be determined by the method shown in Fig. 5.

A hypothetical solidification path shown in a virtual ternary Fe-Zn-F system is plotted for the $N_0$ – nominal solute concentration treated as the starting point, Fig. 6. This solidification path is: $N_0(t_L^{\zeta})\equiv N_0^F \rightarrow N_0(t_C)\equiv N_1$, Fig. 3.

The $N_0$ – nominal solute concentration varies smoothly in the ternary system to reach a constant value on the *liquidus* line of the Fe-Zn binary phase diagram, exactly, when the $t_C$ – time is attended. The flux as well as the product of its combustion do not exist more in the zinc bath. Now, the (Zn) – coating formation follows the solidification path in the Fe-Zn binary phase diagram: $N_1 \rightarrow N^F$. It occurs until the appearance of the first solid-state transformation at a time $t_M \sim 300$ seconds of the galvanizing.

The problem of the length of the solidification path is not fully solved, but it is known that the solidification process combined with diffusion is proceeding in such a way that remaining liquid phase of the $N^F$ – concentration goes into the zinc bath which is of the same concentration. On the other hand, the $N^F$ – equilibrium solution (zinc bath) still serves for the substrate dissolution. The proposed function which describes the kinetics of flux decay, Eq. (1), is used to determine the variability of the peritectic phases concentration during the period of flux existence in the bath. It is shown by the following equations written successively for:

- the variability of zinc concentration in the $\Gamma_1$ – peritectic phase emerging in the sequence as a first one and designated here with the symbol P1;

$$N_{P1}(t)=\begin{cases}k_2 N_1\left(1-F(t)\dfrac{k_2 N_1}{k_2 N_1+k_3 N_2+k_4 N_3}\right), & t_B^{\Gamma 1}\le t\le t_C,\\ k_2 N_1, & t_C\le t,\end{cases} \tag{2}$$

- the variability of zinc concentration in the $\delta$ – peritectic phase emerging in the sequence as a second one and designated here with the symbol P2;

$$N_{P2}(t)=\begin{cases}k_3 N_2\left(1-F(t)\dfrac{k_3 N_2}{k_2 N_1+k_3 N_2+k_4 N_3}\right), & t_B^{\delta}\le t\le t_C,\\ k_3 N_2, & t_C\le t,\end{cases} \tag{3}$$

- the variability of zinc concentration in the $\zeta$ – peritectic phase emerging in the sequence as a third one and designated here with the symbol P3;

$$N_{P3}(t)=\begin{cases}k_4 N_3\left(1-F(t)\dfrac{k_4 N_3}{k_2 N_1+k_3 N_2+k_4 N_3}\right), & t_B^{\zeta}\le t\le t_C,\\ k_4 N_3, & t_C\le t,\end{cases} \tag{4}$$

A consequence of this behavior of the Zn – solute concentration in individual sublayers of the peritectic phases is the variability in the $N_0(t)$ – function, Fig. 7. This function makes the hypothetical solidification path, Fig. 6, defined as well as possible in frame of the present model.

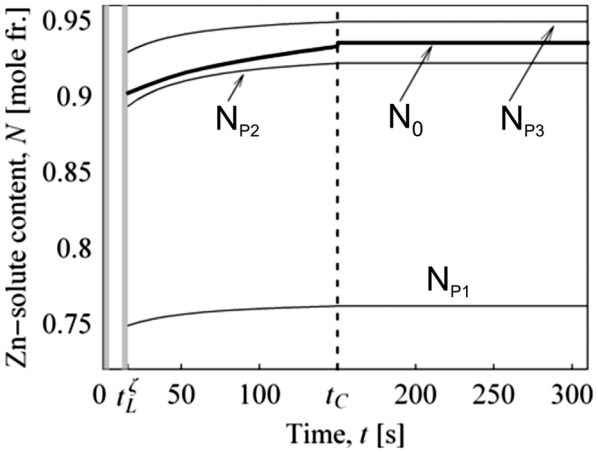


Fig. 7. The variability of zinc concentration in individual sub-layers of the intermetallic phases under the influence of the $F$ – flux, for $t \le t_C$, and after the flux decay, $t > t_C$

The variability of the $N_0$ – parameter is shown more precisely to distinguish the periods of time when the individual nucleus (just born) join each to other to form a fully developed sub-layer. There are two periods: $t_B^{\delta} \div t_L^{\delta}$ and $t_B^{\zeta} \div t_L^{\zeta}$. Both periods of time correspond with grey zones, respectively, Fig. 8. It is to be emphasized that the current model does not operate within the grey zones, Fig. 8.

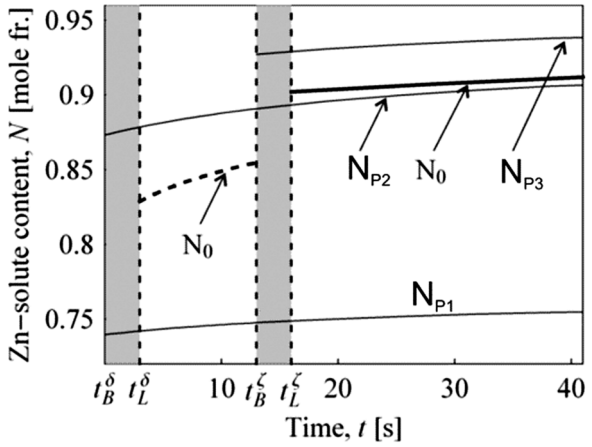


Fig. 8. Area of the model validity; additionally zones: $t_B^{\delta} \div t_L^{\delta}$ and $t_B^{\zeta} \div t_L^{\zeta}$ are distinguished

The definition of the $N_0(t)$ – function is as follows:

- during the flux presence in the zinc bath:

$$N_0^F(t) = \begin{cases} \dfrac{N_{P1}(t)\,\dot{\lambda}^{\Gamma 1}(t) + N_{P2}(t)\,\dot{\lambda}^{\delta C}(t)}{\dot{\lambda}^{\Gamma 1}(t) + \dot{\lambda}^{\delta C}(t)}, & t_L^{\Gamma 1} \le t \le t_B^{\zeta}, \\ \dfrac{N_{P1}(t)\,\dot{\lambda}^{\Gamma 1}(t) + N_{P2}(t)\,\dot{\lambda}^{\delta C}(t) + N_{P3}(t)\,\dot{\lambda}^{\zeta}(t + t_B^{\zeta} - t_B^{\delta})}{\dot{\lambda}^{\Gamma 1}(t) + \dot{\lambda}^{\delta C}(t) + \dot{\lambda}^{\zeta}(t + t_B^{\zeta} - t_B^{\delta})}, & \\ t_L^{\zeta} \le t < t_C, & \end{cases} \quad (5a)$$

- when the flux is evaporated/disappeared:

$$N_0 = \frac{k_3 N_2\,\dot{\lambda}^{\delta}(t) + k_4 N_3\,\dot{\lambda}^{\zeta}(t + t_B^{\zeta} - t_B^{\delta})}{\dot{\lambda}^{\delta}(t) + \dot{\lambda}^{\zeta}(t + t_B^{\zeta} - t_B^{\delta})} = \frac{k_3 N_2\,D + k_4 N_3\,Z}{D + Z}, \qquad t_C \le t \quad (5b)$$

A proper derivatives are present in the above definitions, Eq. (5). This formula corresponds well with the rate of the appropriate phases ($\Gamma_1$, $\delta_C$, $\delta_P$ and $\zeta$), thickening, $\lambda(t)$, which can be calculated on the basis of the laws, $\lambda(t)$, for example, well determined in the industry condition, [23]. Both formulas, however, are generally associated with the data taken from the Fe-Zn phase diagram and additionally with the Lever Rule applied to the peritectic points of this phase diagram.

The compatibility of the solidification path and the results of the solute concentration measurement can be proved while calculating the Zn – solute concentrations of the P1, P2 and P3 – phases which is shown in Fig. 7.

The sum of different growth laws (determined previously for each phase sub-layer, separately, as shown in Fig. 5, for two sub-layers, only) is delivered in Fig. 9.

It also shows the specific sequence of growth, when the whole coating or some of its elements are examined, and not only each sublayer separately. The thick lines are referred to phases growing after the $t_C$ – threshold time, while phases growing in the period of the flux effect are indicated with thin lines, Fig. 9.

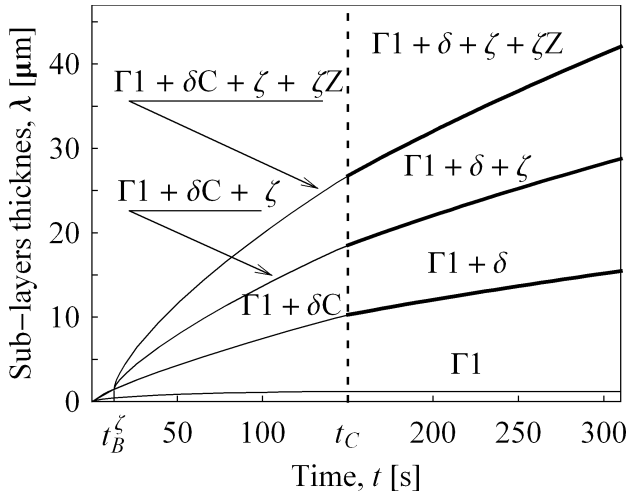


Fig. 9. The growth laws, common for the sums of different phases' sublayers

## 4. Concluding remarks

1 The presence of flux in the zinc bath significantly influences the occurrence of the (Zn) – coating formation for the period of time, $t \le t_C$. First of all, the $\delta \equiv \delta_C$ – peritectic phase has a different morphology in comparison with the $\delta \equiv \delta_P$ – peritectic phase which appears after the flux disappearing. Additionally, the products of the flux decomposition/burning promote the $\zeta$ – phase nucleation and the $\zeta_Z \equiv \zeta + \eta$ – sub-layer appearance. These products act as the substrates for the heterogeneous nucleation of the $\zeta$ – phase.

2 The function which describes the flus disappearing, Eq. (1), allows for presenting the Fe-Zn-F – virtual ternary phase diagram, Fig. 6. According to this ternary phase diagram the solidification path reduces to the path localized on the *liquidus* line for the Fe-Zn – binary phase diagram at the $N_1$ – point well defined in Fig. 3. It proves that the $\Gamma_1$ – phase formation, according to the peritectic reaction, is not possible for the time $t > t_C$, (when the solidification path reaches the $N_1$ – point).

3 Even the sum of the growth laws, Fig. 9, allows for defining the $t_C$ – threshold time at which the flux effect onto the (Zn) – coating formation is completed.

Acknowledgements

**Acknowledgements**

The financial support was provided by the National Center for Research and Development under Grant No. **DEC-2012/05/B/ST8/00100.**

REFERENCES

[1] W. Wołczyński, E. Guzik, D. Kopyciński, C. Senderowski, Mechanism of the Intermetallic Phase/Compound Growth on the Substrate, Journal of Achievements in Materials and Manufacturing Engineering **24**, 324-327 (2007).

[2] A.R. Marder, The Metallurgy of Zinc-Coated Steel, Progress in Materials Science **45**, 191-271 (2000).

[3] R. Parisot, S. Forest, A. Pineau, F. Grillon, X. Démonet, J.M. Mataigne, Deformation and Damage Mechanisms of Zinc Coatings on Hot-Dip Galvanized Steel Sheets, Metallurgical and Materials Transaction **35A**, 797-811 (2004).

[4] J. Inagaki, M. Sakurai, T. Watanabe, Alloying Reactions in Hot-Dip Galvanizing and Galvannealing Processes, ISIJ International **35**, 1388-1393 (1995).

[5] C.R. Xavier, U.R. Seixas, P.R. Rios, Further Experimental Evidence to Support a Simple Model for Iron Enrichment in Hot-Dip Galvanneal Coatings on IF Steel Sheets, ISIJ International **36**, 1316-1327 (1996).

[6] J.D. Culcasi, P.R. Sere, C.I. Elsner, A.R. Sarli, Control of the Growth of Zinc – Iron Phases in the Hot-Dip Galvanizing Process, Surface and Coatings Technology **122**, 21-23 (1999).

[7] W. Wołczyński, E. Guzik, J. Janczak-Rusch, D. Kopyciński, J. Golczewski, H.M. Lee, J. Kloch, Morphological Characteristics of Multi-Layer/Substrate Systems, Materials Characterization **56**, 274-280 (2006).

[8] W. Wołczyński, T. Okane, C. Senderowski, D. Zasada, B. Kania, J. Janczak-Rusch, Thermodynamic Justification for the Ni/Al/Ni Joint Formation by a Diffusion Brazing, International Journal of Thermodynamics **14**, 97-105 (2011).

[9] W. Wołczyński, T. Himemiya, D. Kopyciński, E. Guzik, Solidification and Solid/Liquid Interface Paths for the Formation of Protective Coatings, Archives of Foundry Engineering **6**, 359-362 (2006).

[10] D. Kopyciński, E. Guzik, W. Wołczyński, Coating (Zn) Formation during Hot-Dip Galvanizing, Inżynieria Materiałowa **164**, 289-292 (2008).

[11] D. Kopyciński, TMS 2013 Annual Meeting, Crystallization of Intermetallic Phases Fe-Zn during Hot-Dip Galvanizing Process, TMS2013 Supplemental Proceedings, 439-446.

[12] D. Kopyciński, E. Guzik, Intermetallic Phases Formation in Hot Dip Galvanizing Process, Solid State Phenomena **197**, 77-82 (2013).

[13] D. Kopyciński, A. Szczęsny, The Effect of Ductile Cast Iron Matrix on Zinc Coating during Hot Dip Galvanizing of Castings, Archives of Foundry Engineering **12**, 101-104 (2012).

[14] A. Quiroga, S. Claessens, B. Gay, M. Rappaz, A Novel Experiment for the Study of Substrate-Induced Nucleation in Metallic Alloys, Metallurgical and Materials Transactions **35A**, 3543-3550 (2004).

[15] J. Strutzenberger, J. Faderl, Solidification and Spangle Formation of Hot-Dip Galvanizing Zinc Coatings, Metallurgical and Materials Transactions **29**, 631-646 (1998).

[16] K. Mita, T. Ikeda, M. Maeda, Phase Diagram Study of Fe-Zn Intermetallics, Journal of Phase Equilibria **23**, 1808-1815 (2000).

[17] X. Su, N.Y. Tang, J.M. Toguri, A Study of the Zn-Rich Corner of the Zn-Fe-Sn System, Journal of Phase Equilibria **26**, 528-532 (2003).

[18] W. Xiong, Y. Kong, Y. Dub, L. Zikui, M. Selleby, S. Weihua, Thermodynamic Investigation of the Galvanizing Systems, I: Refinement of the Thermodynamic Description for the Fe-Zn System, Calphad: Computer Coupling of Phase Diagrams and Thermo-Chemistry **33**, 433-440 (2009).

[19] W. Wołczyński, Z. Pogoda, G. Garzeł, B. Kucharska, A. Sypień, T. Okane, Part I. Thermodynamic and Kinetic Aspects of the Hot Dip (Zn) – Coating Formation, Archives of Metallurgy and Materials **59**, 1223-1233 (2014).

[20] W. Wołczyński, J. Janczak-Rusch, Z. Pogoda, Formation of the Ni/Al/Ni Joint Structure Applying an Isothermal Solidification, Archives of Foundry Engineering **8**, 337-342 (2008).

[21] E.P. Kalinushkin, Y. Taran, Effect of Liquid Diffusion on Mechanism of Peritectic Transformation in Alloy Steels, Materials Science Forum **329-330**, 191-196 (2000).

[22] W. Wołczyński, Z. Pogoda, G. Garzeł, B. Kucharska, A. Sypień, T. Okane, Part II. Model for the Protective Coating Formation during Hot Dip Galvanizing, Archives of Metallurgy and Materials **59**, 1393-1404 (2014).

[23] W. Wołczyński, B. Kucharska, G. Garzeł, A. Sypień, Z. Pogoda, T. Okane, Part III. Kinetics of the (Zn) – Coating Deposition during Stable and Meta-Stable Solidifications, Archives of Metallurgy and Materials **60**, 199-207 (2015).

*Received:20 April 2015.*